 doi:10.20944/preprints201912.0297.v1

Article

Concrete-Galvalume Composite Behavior under Elevated Temperatures, Experiment and Numerical Simulation

Agus Maryoto [1], Han Ay Lie [2], and Hendrik Marius Jonkers [3,*]

[1] Department of Civil Engineering, Universitas Jenderal Soedirman, Jl. Mayjend Sungkono KM 5, Blater, Purbalingga, Central Java, Indonesia, 53371; agus_maryoto1971l@yahoo.co.id
[2] Department of Civil Engineering, Diponegoro University, Semarang Indonesia; ayliehan@gmail.com
[3] Department of Civil Engineering and Geoscience, Delf Technical University, Delf-Netherland; h.m.jonkers@tudelft.nl
* Correspondence: agus_maryoto1971@yahoo.co.id; Tel.: (+628112911209.)

Abstract: A galvalume corrugated sheet was utilized as formwork for a reinforced concrete beam in flexure. A numerical model was validated to the experimentally obtained data, and further adopted to simulate the behavior of this composite structure under elevated temperatures. The properties and constitutive stress-strain data of the basic materials were obtained from experiments, and superimposed into the finite element model. The study concluded that the load carrying capacity of the member decreased as a direct function on temperature increase, and the cracking moment was very sensitive to the temperature fluctuation. The elevated temperatures also altered the failure mode.

Keywords: concrete-galvalume composite; elevated temperature; flexure behavior; numerical model; constitutive stress-strain

1. Introduction

The use of floor decks as composite formwork on plate structures (Jiang et al. 2017) has often been done to shorten the completion time of a project. Floor deck, usually made from galvalume steel deck, will be integrated with the concrete plate structure without having to be dismantled and functions as a flexible reinforcement in the area of tensile stress. The beam as a supporting plate is usually cast first then followed by casting the plate on the top of the beam. On the other hand, concrete beam cast using conventional formwork requires dismantling the formwork after the concrete beams have become hard.

The concrete, steel bar as reinforcement and galvalume possess dissimilar thermal conductivity characteristics. Concrete has a thermal conductivity of 0.8 W/mK, while steel has a value of 50.2 W/mK, which is significantly higher than concrete. Aluminum, on the other hand, has a conductivity of 205 Wm/K. The concrete, steel bar as reinforcement and galvalume possess dissimilar thermal conductivity characteristics. Concrete has a thermal conductivity of 0.8 W/mK, while steel has a value of 50.2 W/mK, which is significantly higher than concrete. Aluminum, on the other hand, has a conductivity of 205 Wm/K.

The study of Jiangtao et al., 2011 [1] evaluated the time depended load carrying capacity depreciation of 30 MPa concrete members under fire. The data were recorded for a burning period of 60 and 75 minutes, which for the purpose of evaluation in this study were converted to a temperature of 349^{o} and 405^{o}C. Mundhada and Pofale, 2015 [2] experimentally evaluated 25 MPa reinforced concrete (RC) beams to an elevated temperature of 550^{o}, 750^{o} and 950^{o}C, while Kiute et al., 2014 [3] executed tests on Class 20 and Class 25 beams for a period of one and two hours under a constant

Preprints (www.preprints.org) | NOT PEER-REVIEWED | Posted: 22 December 2019 doi:10.20944/preprints201912.0297.v1

temperature of 250°, 600° and 700°C. The data were normalized to the room temperature specimen's values for comparison and the trends were established as a function of temperature. It is seen that the composite galvalume member has a more intensive reduction rate.

The compressive strength of concrete reduced around 20% when the concrete exposed on temperature 300°C [4]. Unfortunately, the behavior of composite concrete beams with galvalume as formwork under elevated heat has not yet been rarely examined. Acknowledging the outstanding resilience towards heat, research was conducted to numerically picture the behavior of this section under elevated temperatures. The simulation compared the moment-deformation response and failure mode of the beams under a temperature of 25° (room temperature), 100°, 200° and 300°C. Therefore, this study aims to determine the behavior of galvalume composite concrete beams against bending loads at elevated temperatures using numerical simulation.

2. Methods

2.1. Specimens and type of testing

A finite element model (FEM) of the specimen under consideration was constructed. All material properties obtained from the laboratory tests functioned as input to the model. The conventional reinforcing elements were assumed as fully bonded to the concrete. Analogously, the galvalume was designed to have a complete compatibility with the concrete as well. The non-linear software ATENA was utilized in extracting the data. The model was subjected to a monotonic displacement increment of 0.5 mm.

The stress-strain relationship of concrete was based on the following (Fig. 1a). The concrete in tension is assumed to crack at a stress level of $f_t^{'ef}$. The initial crack propagates under the increasing load, widens and reaches an ultimate strain at ε_o. The crack propagation scheme is shown in Fig. 1b. The concrete in compression initially undergoes crushing at the nodes when stresses reach $f_c^{'ef}$ corresponding to a strain of ε_c. Failure takes place when strains reach the ultimate concrete strain ε_d. The decrease in material stiffness was incorporated based on the secant modulus of elasticity. To accommodate the confinement effect in bi-axial compression, the *Kupfer-Hilsdorf-Rüsch* failure criterion was employed. The steel and galvalume bi-axial responses were accommodated through the *Von Misses* failure envelope. The steel and galvalume constitutive model followed a bi-linier path.

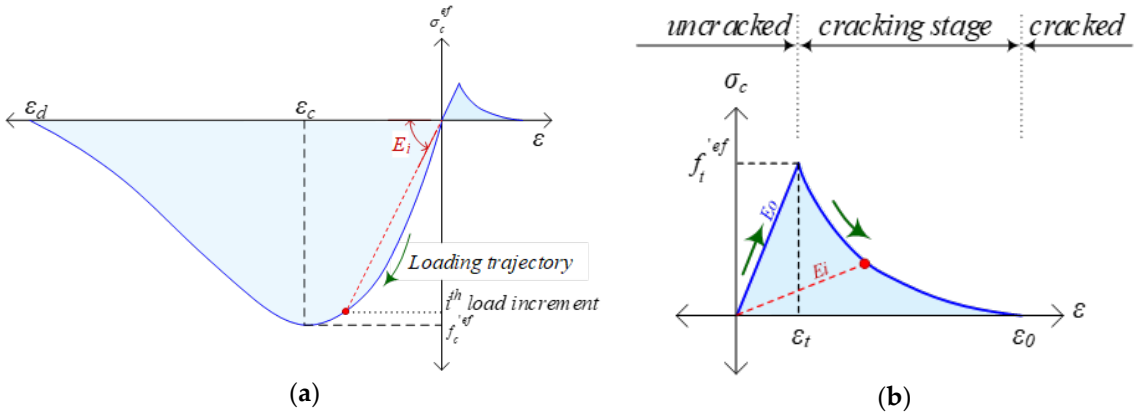

Figure 1. Constitutive model of concrete: (**a**) Compression and tension constituve model of concrete; (**b**) Crack propagation.

To enable the simulation of the beam's behavior under elevated temperatures, the properties of the basic materials – concrete, reinforcing steel and galvalume – were required. The temperature influence on the material properties of concrete has been studied to great length [5,6,7,8,9,10]. Generally, both the compression and the tensile strength decrease as temperature increases. The constitutive model and failure envelope were numerically modified based on these findings [11,12].

The loading in this research was generated by a two-point loading system, creating a pure bending state in between the loading points. The load was applied with a constant displacement

Preprints (www.preprints.org) | NOT PEER-REVIEWED | Posted: 22 December 2019 doi:10.20944/preprints201912.0297.v1

increment of 0.5 mm; this pattern was adopted in the FEM. The work resulted in, among others, the moment versus vertical displacement at midpoint of the member. From the test results, the initial cracking of concrete in tension, as well as the yielding of steel bars, were obtained. The results were counter checked with the data reading from the strain gauges situated at the maximum bending moment location. The two specimens showed a similar trajectory and were almost identical. This moment-displacement curve was used to validate the FEM. To ensure a good comparison, material properties and loading conditions were adopted precisely.

A three-dimensional solid model was discreetly meshed using eight-node hexahedral elements (Fig. 2), with each node having 3 DOF. Boundary conditions were provided at the supports, restraining node movements in the Y and Z directions. The nodes that simulated the support were situated at a distance of 80 mm from the end of the beam, following the experimental specimens' set-up. The load was applied at a distance of 760 mm from the support, dividing the unsupported beam-length into three equal segments. The load was acting on the top nodes, creating a constant displacement increment. All elements were transformed from the global coordinate system to natural coordinates, as can be seen in Fig. 2.

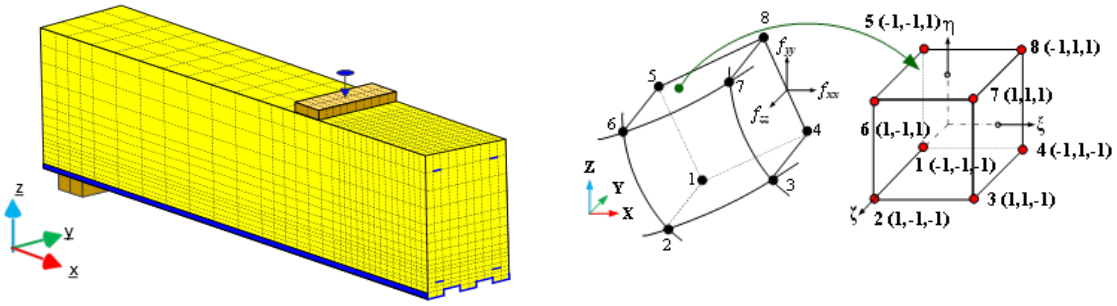

Figure 2. Eight-node hexahedral meshing and element details of the beam.

Due to the symmetric nature of the specimen, one-half of the beam was modeled to conserve running time. An *h*-refinement was applied to the area of interest enabling a more precise stress evaluation in these regions.

There are four specimens in the numerical simulation which are BGFEM, BGFEM100, BGFEM200 and BGFEM300. In these syimbol BG is for Beam Galvalum, FEM is Finite Element Method, number behind the BGFEM is representation of temperature value which are 25°C, 100°C, 200°C and 300°C.

2.2. Experimental procedures

The specimen of concrete galvalume-composite beam is investigated by applying bending load at room temperature around 25°C [13]. The result data were assessed to validate the numerical simulation result of the galvalume-composite beam at room temperature. The section of beam under consideration is a 200 by 300 mm member with a corrugated bottom formwork consisting of a 1 mm thick galvalume sheet. The member was a simply supported beam with a length of 2.44 meters. Galvalume is a steel sheet with a galvanized layer of zinc and aluminum. In terms of working speed and service time improvements, this method provides an excellent enhancement. Further, the presence of galvalume contributed to the member's load carrying capacity, due to the additional tensile vector in the section's tensile area. The zinc provides excellent corrosion and alkali resistance while the aluminum contributes to durability, acid and heat resistance. The positive contribution of these sheets was confirmed by Bailey et al., 2000 [14].

The material has a yield stress of 300 MPa, a yield strain of 0.0015 and a Young's modulus of 100 GPa. Galvalume has a remarkably ductile nature, with an ultimate yield strain reaching 0.17. The stress-strain relationship follows a bi-linear pattern. The concrete has a 28-day cylindrical compression strength of 20 MPa. The material properties and the cross-section of the specimens are shown in Fig. 3a and Fig. 3b. The test results demonstrated that a significant increase in load carrying

Preprints (www.preprints.org) | NOT PEER-REVIEWED | Posted: 22 December 2019 doi:10.20944/preprints201912.0297.v1

capacity was obtained through the use of the corrugated formwork. The yield moment ratio between the composite and conventional section was measured to be 2.45, while the ductility factor increased from 3.9 to 5.3.

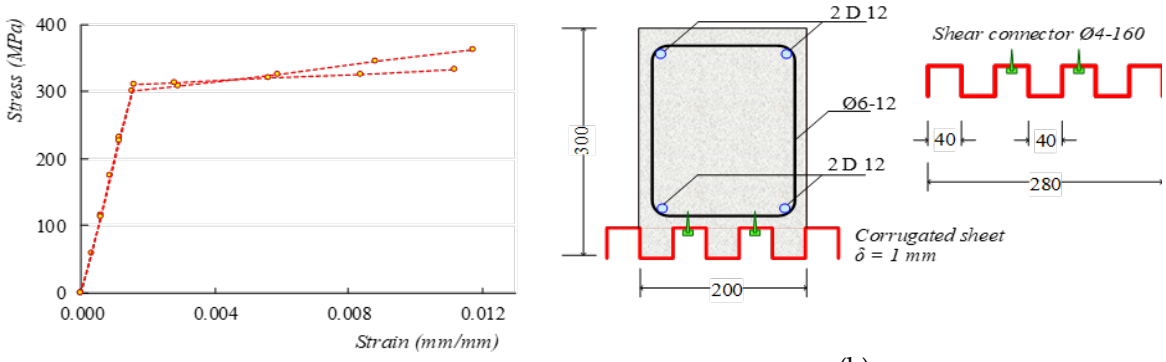

(a) (b)

Figure 3. Galvalume properties and dimension: (a) Galvalume stress-strain properties; (b) Galvalume cross section and dimension.

In order to obtain the physical properties, galvalum was tested under elevated temperature which was applied in the numerical simulation. The effect of temperature elevations to galvalume corrugated sheets were scarcely investigated since this material has a broad range of variations galvanizing material properties. The material properties of the galvalume material used in this study thus had to be obtained through experimental tests. Assuming a linear stress-strain response, the sheets were subjected to a temperature of 100°, 200° and 300°C over a period of one hour. The temperature was carefully monitored using an infrared sensor gun and the specimens were tested under elevated temperature. Additionally, the conductivity of the composite material was monitored to obtain data on the temperature incongruence prior to heat exposure. The embedded tensile reinforcement was assumed to have equivalent temperatures to the surrounding concrete. An analog method was used for the reinforcing steel bars, based on the research work [15,16,17,18,19]. Another experimental test, Scanning Electron Microscope (SEM), was also carried out to correlate the physical and mineralogic change of the galvalume and mechanical properties.

3. Results and Discussion

3.1. Material properties under elevated temperature

The tensile strength and modulus of elasticity of galvalume, steel bar as reinforcement, and concrete is shown in the Table 1. Based on the data, it can be seen that when the temperature increase, both the tensile strength and modulus of elasticity decrease significantly. These data were used as physical and mechanical properties input in the numerical simulation.

Table 1. Material properties under various temperatures.

Temperature	Galvalume		Temperature	Reinforcement		Concrete	
(°C)	f_y (MPa)	E_s (GPa)	(°C)	f_y (MPa)	E_s (GPa)	f_y (MPa)	E_s (GPa)
25	305	19.70	22	400	19.17	19.7	21.63
100	225	64.16	55	340	16.29	19.4	21.52
200	140	15.82	80	252	12.08	19.2	21.45
300	55	3.90	170	200	9.58	18.3	21.10

3.2. Flexure strength

Preprints (www.preprints.org) | NOT PEER-REVIEWED | Posted: 22 December 2019 doi:10.20944/preprints201912.0297.v1

The FEM model was validated to the experimental data. The moment-displacement curves measured at the section's bottom fibers at mid-point were compared, and important information such as first cracking of concrete in tension and steel yielding were detected and assessed against the laboratory results. In achieving the most appropriate meshing configuration, a sensitivity analysis was performed on the cracking, as well as yielding moment and its corresponding displacement. The optimum meshing formation was decided upon the reaching of a convergence state. Finer meshing beyond this number would barely improve the outcome but significantly enhance running time. Since the model was replicating the experimentally tested beam, the displacement increment was synchronized to the actual behavior. The resulting moment-displacement curve is shown in Fig. 4a. The two experimental databases were denoted BGex1 and BGex2, while the FEM model was designated as BGFEM.

The trajectory result of the FEM presents a remarkably close representation to the actual behavior (Fig. 4a). The specimen's response was initially linear until concrete cracking in the tension zone. The FEM had an initial stiffness of 12.5 kNm/mm, while the initial stiffness of BGex was 11.5 kN/mm. The model detected the first crack at a moment of 25 kN-m, while the GBex first crack was found at 23 kN-m, based on the strain gauge readings. The FEM resulted in a slightly higher moment value and a marginally greater initial stiffness. Yield of the BGFEM was recorded at 46.4 kN-m, corresponding to a displacement of 12.0 mm. The experimental specimen BGex yielded at 45.8 kN-m with a deflection of 16.1 mm.

The main origin of these deviations originates from the assumption that in the FEM a full bond exists between the galvalume sheets and the concrete, whereas the test results illustrated debonding between the concrete and the sheet at some point during loading. However, with a difference of not more than 13%, the model was established to be sophisticated enough to be further used as a tool in evaluating the elevated temperature effects.

The bending moment of concrete-galvalume composite under elevated temperature are presented in Fig. 4b. It can be seen that the temperature rise influences the performance of the member negatively. Numerous research results on slabs with corrugated sheets have confirmed this outcome [20,21,22,23]. The cracking and yielding moments and displacements are listed in Table 2.

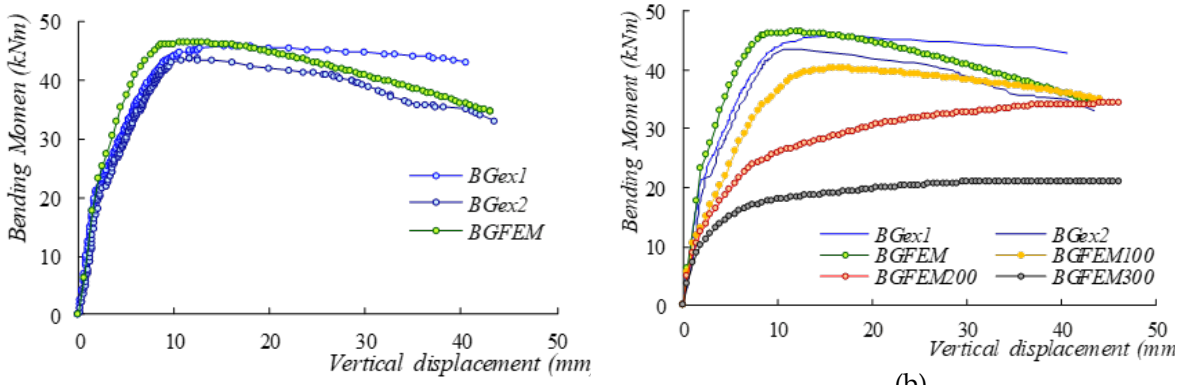

Figure 4. FEM validation and elevated temperature effects on the momen-displacement: (a) Model validation; (b) Momen-displacement response.

The data demonstrated that the elevation in temperature accelerates the cracking and the yield moment. These events also occurred at a much lower displacement degree. The beams subjected to 200^{0}C and 300^{0}C, however, expressed a different pattern. No distinguished yielding point was detected, and the beams continued to deform with a mild rising, almost flat branch. All four specimens' failure modes were characterized by crushing of concrete in the compression zone. The galvalume, due to its very high ductility, could sustain very large deflections and postponed the collapse of the element. This outcome is underlined by the test results on slabs with corrugated steel decks [24,25,1]. Experimental test results on prestressed composite beam showed similar deformation responses [25]. The fact that all strength parameters of concrete, steel bar, and galvalume decreased

Preprints (www.preprints.org) | NOT PEER-REVIEWED | Posted: 22 December 2019 doi:10.20944/preprints201912.0297.v1

as a function of increasing temperature, explained the acceleration of the cracking as well as yielding moments as well as the reduction of initial stiffness.

Table 2. Momen-displacement data.

Temperature exposure	Cracking moment M_{cr} (kN-m)	Displacement (mm)	Yield moment M_y (kN-m)	Displacement (mm)	Initial Stiffness (kNm/mm)
BGFEM	25.46	2.5	46.38	12.0	12.5
BGFEM100	11.84	1.5	40.29	16.0	11.5
BGFEM200	10.64	1.5	34.42	-	9.8
BGFEM300	8.91	1.5	21.14	-	7.6

The capacity depreciation response as a function of temperature intensification is presented in Fig. 5a, while Fig. 5b represents a comparison to reinforced concrete conventional members.

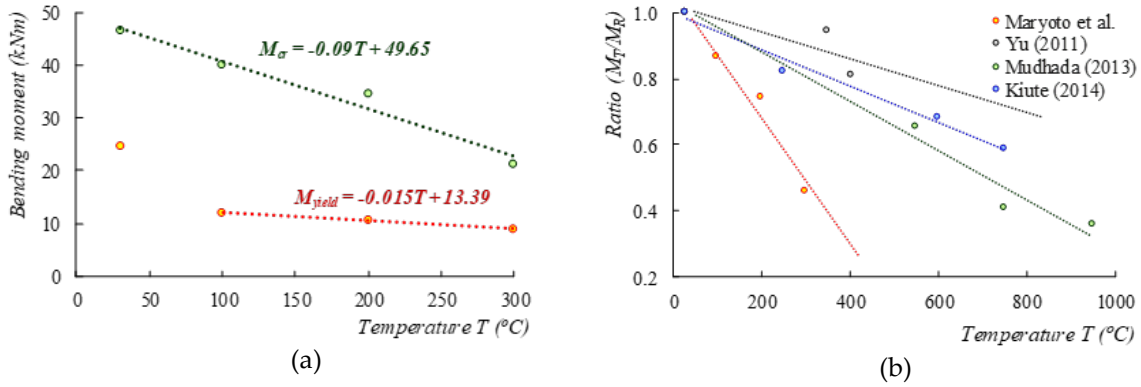

(a) (b)

Figure 5. Temperature response to the moment capacity: (a) Concrete-Galvalume moment response; (b) Comparison to RC beams.

The influence of elevated temperatures to the moment capacity follows a linear relationship. The rate of decrease of the cracking moment, is more pronounced than the rate of decrease for the yielding moment. The reason for this behavior originates from the fact that the increase in temperature has stronger effects on concrete than steel. The yield data for the room temperature specimen detected as an outlier was taken out of the equation (Fig. 5a).

The stresses were evaluated at a deflection of 10 mm, in correlation with the maximum allowable deflection of $\frac{1}{240}L$ in accordance with ACI standards [26]. The stress concentrations and cracks as predicted by the FEM are shown in Fig. 6a and 6b.

The specimen BGFEM has intense stress and concentrations localized at the maximum flexure zone. Shear-flexure cracks developed in the maximum shear zone and were confirmed by visual observation on the laboratory tested beams. The BGFEM300^0 had a much broader stress-strain distribution, with lower overall stress levels, due to the degradation in strength and stiffness of the materials. The tensile stresses proliferated to the areas within the maximum flexure zone due to the premature yielding of galvalume and steel. Extensive cracking was present, and in the vicinity of the load, flexure-shear cracks began to form.

Preprints (www.preprints.org) | NOT PEER-REVIEWED | Posted: 22 December 2019 doi:10.20944/preprints201912.0297.v1

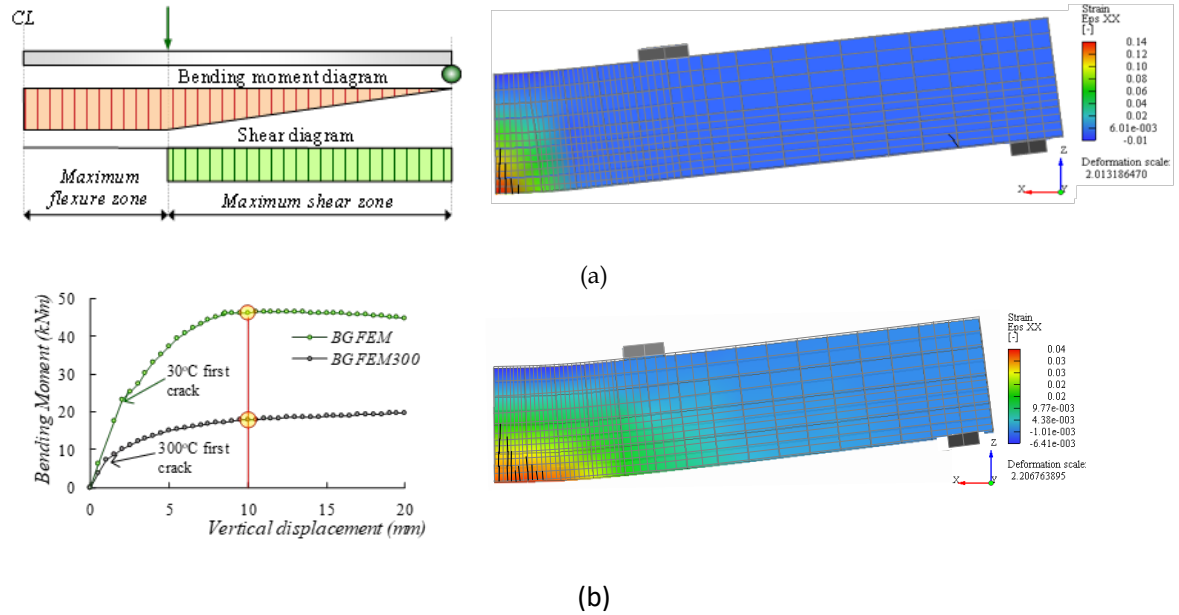

Figure 6. Stress concentrations and cracking: (a) Stress concentrations at 30°C (BGFEM32); (b) Stress concentrations at 300°C (BGFEM32300).

3.3. *Galvalume scanning electron microscope (SEM)*

The SEM analyses on the physical appearance of galvalume sheets prior and after tensile testing at room temperature and 100°C are displayed in Fig. 7a and 7b, respectively. The micrographs demonstrate that the elevated temperatures and tensile stresses altered the molecular configuration. Large gaps between the materials were detected, measuring up to 4 μm for the room temperature specimens after tensile failure (Fig. 7a). Heating of the galvalume also modified the physical structure. The chemical analyses on the surfaces showed that the zinc coating was significantly diminished, leaving the steel exposed. In Fig. 7b, a smooth facetted surface measuring up to 5 by 2 μm is seen. The heating process also reduces the carbon content on the surface. Upon testing, the process yielded a homogeneous mass.

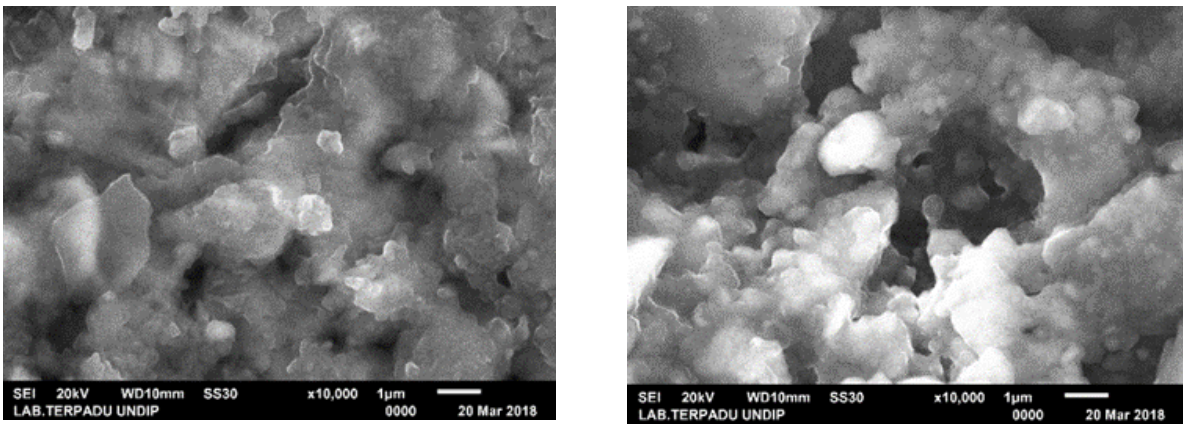

Preprints (www.preprints.org) | NOT PEER-REVIEWED | Posted: 22 December 2019 doi:10.20944/preprints201912.0297.v1

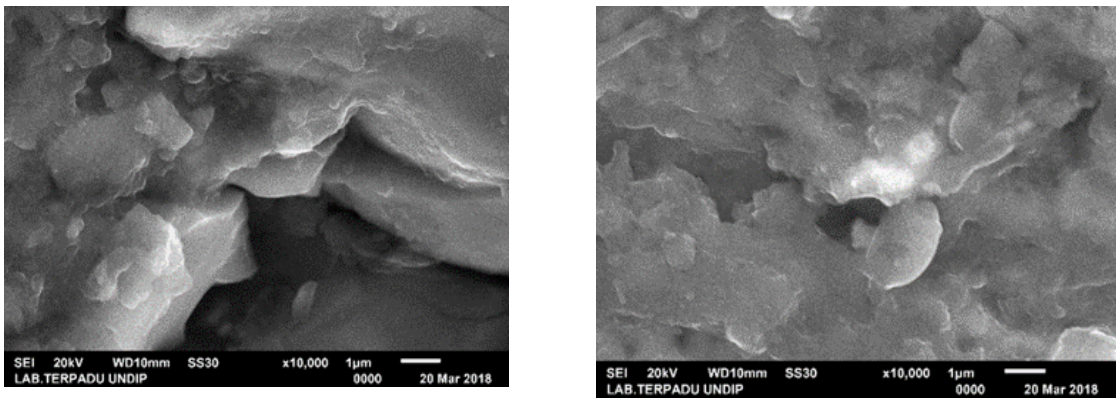

Figure 7. SEM reading on Galvalume material: (a) Room temperature Galvalume prior to (left) and after (right) tensile testing; (b) Galvalume exposed to 100°C prior to (left) and after (right) testing

4. Conclusions

The composite concrete-galvalume beam has excellent performance, both in load carrying capacity aspects, as well as in its ductility behavior. A FEM was constructed to model the beam based on the eight-node hexahedral element. The model's output showed a remarkable resemblance to the behavior of the actual laboratory tested specimen. The FEM had a slightly higher stiffness throughout its loading sequence. The origin of this divergence was the incorrect assumption of a full-bonded condition between the galvalume and the concrete. The degree of compatibility should therefore be determined more precisely, based on experimentally tested shear connectors exposed to elevated temperatures [27].

The SEM readings clearly showed the change in the chemical as well as physical conditions of the galvalume surface. The unheated sheets were characterized by the presence of small fractures within the material, while the heated elements had a more homogeneous surface.

The model was expanded to simulate the moment-displacement behavior of this beam under elevated temperatures. It was found that the diminution in load carrying capacity was a direct, linear function to the temperature fluctuation. The cracking moment was more susceptible to temperature rise, due to the sensitive nature of the tensile strength of concrete. The research outcome is also a factor of the original material properties and the dimension of the cross-section [28]; the model could hence be expanded to accommodate the variables within this corridor.

The flexure stress concentrations of the un-elevated specimen BGFEM were condensed at the center of the beam. Shear-flexure cracks formed in the maximum shear area. The heating process shifted the stress concentrations of the heated beam BGFEM300, extending outside the maximum flexure zone. No shear or shear-flexure cracks were detected in the maximum shear area. The stresses in this element were relatively lower than the BGFEM, as a result the specimens stiffness decreased. The alteration in failure mode was the result of disproportional material behavior change due to elevated temperatures.

Author Contributions: conceptualization, Agus Maryoto and Han Ay Lie.; methodology, Agus Maryoto and Han Ay Lie.; software, -.; validation, Han Ay Lie., Hendrik Marius Jonkers.; formal analysis, Agus Maryoto.; investigation, Agus Maryoto.; resources, Agus Maryoto.; data curation, Agus Maryoto.; writing—original draft preparation, Agus Maryoto; writing—review and editing, Agus Maryoto; visualization, Agus Maryoto; supervision, Agus Maryoto.; project administration, Agus Maryoto; funding acquisition, Agus Maryoto".

Funding: This research was funded by Authors.

Acknowledgments: Thank you to Civil Engineering Laboratory of Diponegoro University Team for the support to conduct this research.

Conflicts of Interest: The authors declare no conflict of interest. The funders had no role in the design of the study; in the collection, analyses, or interpretation of data; in the writing of the manuscript, or in the decision to publish the results.

References

1. Jiangtao, Y.U.; Zhaoudao, L.U.; and Xiang K. Experimental Study on the Performance of RC Continuous Members in Bending after Exposure to Fire. Proc Eng 2011;14;821-829. DOI: 10.1016/j.proeng.2011.07.104.
2. Mundhada, A.R.; and Pofale, A.D. Effect of high temperature on compressive strength of concrete. IOSR J Mech Civ Eng. 2015:12(1); 66-70. DOI: 10.9790/1684-12126670.
3. Kiute, L.M.; Mang'uriu, G.N.; and Mulu, P. Effects on Flexural Strength of Reinforced Concrete Beams Subjected to Fire. Civ Env Res. 2014:6(11):36-45.
4. Antonius; Widhianto, A.; Darmayadi, D.; and Asfari, G.D. Fire Resistane of Normal and High-Strength Concrete with Contains of Steel Fibre. Asian J Civ Eng, 2014:15(5); 655-669.
5. Chang, Y.F.; Chen, Y.H.; Sheu, M.S.; and Yao, G.C. Residual stress-strain relationship for concrete after exposure to high temperatures. Cem Conc Res 2006:36;999–2005, DOI: 10.1016/j.cemconres.2006.05.029.
6. Netinger, I.; Kesegic, I.; and Guljas, I. The effect of high temperatures on the mechanical properties of concrete made with different types of aggregates. Fire Saf J 2011:46(7);425-430, DOI: 10.1016/j.firesaf.2011.07.002.
7. Mundhada A.R., and Pofale A.D. (2013). "Effect of elevated temperatures on performance of RCC beams." International Journal of Civil, Structural, Environmental and Infrastructure Engineering Research and Development, Vol. 3, No.3, pp. 105-112.
8. Ma, Q.; Guo, R.; Zhao, Z.; Lin, Z.; and He, K. Mechanical properties of concrete at high temperature-A review. Construction and Building Materials, 2015:93;371-383, DOI: 10.1016/j.conbuildmat.2015.05.131.
9. Pazdera, L.; Topolar, L.; Mikulasek, K.; Smutny, J.; and Seelmann, H. Non-Linear Characteristics of Temperature Degraded Concrete at High Temperature. Proc Eng 2017:190;100-105, DOI: 10.1016/j.proeng.2017.05.313.
10. Guruprasad, Y.K.; and Ramaswamy, A. Micromechanical analysis of concrete and reinforcing steel exposed to high temperature. Constr Build Mat 2018:158;761-773, DOI: 10.1016/j.conbuildmat.2017.10.061.
11. Guo, S. Experimental and numerical study on restrained composite slab during heating and cooling. J Constr Steel Res 2012:69(1);95–105, DOI: 10.1016/j.jcsr.2011.08.009.
12. Jiang, J.; Main, J.A.; Weigand, J.M.; and Sadek, F.H. Thermal performance of composite slabs with profiled steel decking exposed to fire effects. Fire Saf J 2018:95;25-41, DOI: 10.1016/j.firesaf.2017.10.003.
13. Priastiwi, Y.A.; Han, A.L.; Maryoto, A.; and Noor, E.S. Experimental study on the use of steel-decks for prefabricated reinforced concrete beams. IOP Conf: Mat Sci Eng 2017:271;1-8, DOI: 10.1088/1757-899X/271/1/012095.
14. Bailey, C.G.; White, D.S.; and Moore, D.B. The tensile membrane action of unrestrained composite slabs simulated under fire conditions. Eng Struc 2000:22;1583–1595. DOI: 10.1016/S0141-0296(99)00110-8.
15. Chen, J.; and Young, B. Stress-strain curves for stainless steel at elevated temperatures. Eng Struc 2006:28(2);229–239. DOI: 10.1016/j.engstruct.2005.07.005.
16. Robert, M.; and Benmokrane, B. Behavior of GFRP Reinforcing Bars Subjected to Extreme Temperatures. J Com Constr 2010:14(4);353-360. DOI: 10.1061/(ASCE)CC.1943-5614.0000092.
17. Gardner, L.; Bu, Y.; Francis, P.; Badoo, N.R.; Cashell, K.A.; and McCann, F. Elevated temperature material properties of stainless steel reinforcing bar. Const Build Mat 2016:114;977–997. DOI: 10.1016/j.conbuildmat.2016.04.009.
18. Cai, W.; Morovat, M.A.; and Engelhardt, M.D. True stress-strain curves for ASTM A992 steel for fracture simulation at elevated temperatures. J Constr Steel Res 2017:139;272-279. DOI: 10.1016/j.jcsr.2017.09.024.
19. Tao, Z.; Wang, X.Q.; Hassan. M.K.; Song, T.Y.; and Xie, L.A. Behaviour of three types of stainless steel after exposure to elevated temperatures. J Constr Steel Res 2018: In press, corrected proof, Available online 3 March 2018.
20. Bednář, J.; Wald, F.; Vodička, J.; and Kohoutková, A. Experiments on membrane action of composite floors with steel fibre reinforced concrete slab exposed to fire. Fire Saf J 2013:59;111-121. DOI: 10.1016/j.firesaf.2013.04.008.
21. Jiang, J.; Main, J.A.; Sadek, F.; and Weigand, J.M. Numerical Modeling and Analysis of Heat Transfer in Composite Slabs with Profiled Steel Decking. 2017: NIST Technical Note 1958, National Institute of Standards and Technology, Gaithersburg, MD.
22. Jiang, J.; Joseph, A.M.; Jonathan, M.W.; and Fahim, H.S. Thermal performance of composite slabs with profiled steel decking exposed to fired effects. Fire Saf J 2017:95;24-41. DOI: 10.1016/j.firesaf.2017.10.003.

23. Nguyen, M.P.; Nguyen, T.T.; and Tan, K.H. Temperature profile and resistance of flat decking composite slabs in- and post-fire. Fire Saf J 2018:98;109-119. DOI: 10.1016/j.firesaf.2018.04.001.
24. Li, G.Q.; Zhang, N.; and Jiang, J. Experimental investigation on thermal and mechanical behaviour of composite floors exposed to standard fire. Fire Saf J, 2017:89;63-76. DOI: 10.1016/j.firesaf.2017.02.009.
25. Zhou, H.; Li, S.; and Zhang, C. Fire tests on composite steel-concrete beams prestressed with external tendons. J Constr Steel Res 2018:143;62-71. DOI: 10.1016/j.jcsr.2017.12.008.
26. ACI 318. Building code requirements for structural concrete (ACI 318-14) and commentary, ACI 318-14, American Concrete Institute 2014: Farmington Hills, MI, USA
27. Mashiri, F.R.; Mirza, O.; Canuto, C.; and Lam, D., Post-fire Behaviour of Innovative Shear Connection for Steel-Concrete Composite Structures. Structures, 2017: 9;147-156. DOI: 10.1016/j.istruc.2016.12.001.
28. Nguyen, T.T.; and Tan, K.H. Behaviour of composite floors with different sizes of edge beams in fire. J of Constr Steel Res 2017:129;28-41. DOI: 10.1016/j.jcsr.2016.10.018.